

# Axial Shielding of 5d<sup>8</sup> and 5d<sup>7</sup> Metal Centers in Dimesitylplatinum Complexes with Unsaturated Chelate Ligands: Spectroscopic and Spectroelectrochemical Studies of Four Different Oxidation States

Axel Klein and Wolfgang Kaim\*

Institut für Anorganische Chemie der Universität Stuttgart,  
Pfaffenwaldring 55, D-70550 Stuttgart, Germany

Received August 1, 1994<sup>®</sup>

Platinum(II) complexes (N<sup>∧</sup>N)PtMes<sub>2</sub>, Mes = mesityl, were synthesized with the α-dimine chelate ligands N<sup>∧</sup>N = 2,2'-bipyridine, 2,2'-bipyrazine, 2,2'- and 4,4'-bipyrimidine, 1,4,7,10-tetraazaphenanthrene, and dipyrido[3,2-a:2',3'-c]phenazine. The compounds can be reversibly reduced to EPR and UV/Vis/near-IR spectroelectrochemically detectable radical complexes [(N<sup>∧</sup>N<sup>•-</sup>)Pt<sup>II</sup>Mes<sub>2</sub>]<sup>-</sup> and to dianions [(N<sup>∧</sup>N<sup>••-</sup>)Pt<sup>II</sup>Mes<sub>2</sub>]<sup>2-</sup>. Reversible one-electron oxidation is also possible, leading to cations [(N<sup>∧</sup>N)Pt<sup>III</sup>Mes<sub>2</sub>]<sup>+</sup>, which are EPR-silent even at 4 K but exhibit the typical ligand-field transitions for planar low-spin d<sup>7</sup> ions. The unusual persistence of the Pt(III) state results from an effective protection of the axial positions by two mesityl groups which also block oxidative addition reactions. In contrast, the complexes (bpy)PtClMes and (bpy)Pt(o-CF<sub>3</sub>Ph)<sub>2</sub>, o-CF<sub>3</sub>Ph = o-(trifluoromethyl)phenyl, have better accessible axial positions and are no longer oxidized reversibly. In agreement with the spectroelectrochemical results for the singly oxidized and reduced states, the neutral precursor molecules are distinguished by low-lying MLCT excited states which give rise to solvatochromic absorption and emission features. Comparison of the data from optical spectroscopy and from reversible one-electron redox processes allowed us to determine the solvent-dependent contributions from intra- and intermolecular reorganization following MLCT excitation.

Complexes of platinum(II) are generally distinguished by high substitutional stability and by a square planar coordination geometry at the metal center. These compounds have received much attention because of their prototypical oxidative addition reactivity,<sup>1,2</sup> their aggregation tendencies,<sup>3</sup> their therapeutical potential,<sup>4</sup> and their photophysical properties, in particular their often intense luminescence.<sup>5</sup> Light-emitting Pt(II) complexes frequently contain π-acceptor ligands, and the resulting metal-to-ligand charge transfer (MLCT) excited states are thus available for emission.<sup>2e,5</sup> However, the presence of the 5d element platinum in such complexes causes a complicated electronic situation because of the high spin-orbit coupling constant of the element and because of the possible interaction of 5d and 6s metal orbitals with ligand MOs.<sup>5f,g</sup> Furthermore,

the coordinatively unsaturated square planar situation invites aggregation, e.g., via Pt-Pt contacts or other stacking interactions.<sup>3,5a,i,k,q</sup> It is not surprising, therefore, that intermolecular interactions have to be considered in the photo-<sup>5a,i,k,q</sup> and electrochemistry of Pt(II) systems; for instance, the removal of one electron from Pt(II) usually proceeds irreversibly<sup>2e</sup> due to the attack by nucleophiles in the axial position of the thus primarily obtained Pt(III) species. In contrast to low-spin d<sup>8</sup> states, the low-spin d<sup>7</sup> configuration generally favors

<sup>®</sup> Abstract published in *Advance ACS Abstracts*, January 15, 1995.

(1) Collman, J. P.; Hegedus, L. S.; Norton, J. R.; Finke, R. G. *Principles and Applications of Organotransition Metal Chemistry*; University Science Books: Mill Valley, CA, 1987; Chapter 5.

(2) (a) Chaudhury, N.; Puddephatt, R. J. *J. Organomet. Chem.* **1975**, *84*, 105. (b) Scott, J. D.; Puddephatt, R. J. *Organometallics* **1986**, *5*, 1538. (c) Aye, R. J.; Ferguson, G.; Lough, A. J.; Puddephatt, R. J. *Angew. Chem.* **1989**, *101*, 765; *Angew. Chem., Int. Ed. Engl.* **1989**, *28*, 767. (d) Achar, S.; Puddephatt, R. J. *Angew. Chem.* **1994**, *106*, 895; *Angew. Chem., Int. Ed. Engl.* **1994**, *33*, 847. (e) Vogler, C.; Schwederski, B.; Klein, A.; Kaim, W. *J. Organomet. Chem.* **1992**, *436*, 367.

(3) (a) Krogmann, K.; Hausen, H.-D. *Z. Anorg. Allg. Chem.* **1968**, *358*, 67. (b) Thomas, T. W.; Underhill, A. E. *Chem. Soc. Rev.* **1972**, *1*, 99. (c) Gencheva, G.; Mitewa, M.; Bontchev, P. R.; Gochev, G.; Macicek, J.; Zhecheva, E.; Yordanov, N. D. *Polyhedron* **1992**, *11*, 365. (d) Coyer, M. J.; Herber, R. H.; Chen, J.; Croft, M.; Szu, S. P. *Inorg. Chem.* **1994**, *33*, 716. (e) Harvey, P. D.; Truong, K. D.; Aye, K. T.; Drouin, M.; Bandrauk, A. D. *Inorg. Chem.* **1994**, *33*, 2347. (f) Herber, R. H.; Croft, M.; Coyer, M. J.; Bilash, B.; Sahiner, A. *Inorg. Chem.* **1994**, *33*, 2422.

(4) (a) Sundquist, W. I.; Lippard, S. J. *Coord. Chem. Rev.* **1990**, *100*, 293. (b) Lippert, B. *Prog. Inorg. Chem.* **1989**, *37*, 1.

(5) (a) Miskowski, V. M.; Houlding, V. H. *Inorg. Chem.* **1989**, *28*, 1529. (b) Ballardini, R.; Gandolfi, M. T.; Prodi, L.; Ciano, M.; Balzani, V.; Kohnke, F. H.; Zavareh, H. S.; Spencer, N.; Stoddart, J. F. *J. Am. Chem. Soc.* **1989**, *111*, 7072. (c) Zuleta, J. A.; Chesta, C. A.; Eisenberg, R. J. *Am. Chem. Soc.* **1989**, *111*, 8916. (d) Che, C.-M.; Wan, K.-T.; He, L.-Y.; Poon, C.-K.; Yam, V. W.-W. *J. Chem. Soc., Chem. Commun.* **1989**, 943. (e) Che, C.-M.; He, L.-Y.; Poon, C.-K.; Mak, C. W. *Inorg. Chem.* **1989**, *28*, 3081. (f) Biedermann, J.; Gliemann, G.; Klement, U.; Range, K.-J.; Zabel, M. *Inorg. Chem.* **1990**, *29*, 1884. (g) Biedermann, J.; Gliemann, G.; Klement, U.; Range, K.-J.; Zabel, M. *Inorg. Chim. Acta* **1990**, *169*, 63. (h) Kunkely, H.; Vogler, A. *J. Am. Chem. Soc.* **1990**, *112*, 5625. (i) Wan, K.-T.; Che, C.-M.; Cho, K.-C. *J. Chem. Soc., Dalton Trans.* **1991**, 1077. (k) Miskowski, V. M.; Houlding, V. H. *Inorg. Chem.* **1991**, *30*, 4446. (l) Vogler, A.; Kunkely, H. *Angew. Chem.* **1982**, *94*, 217; *Angew. Chem., Int. Ed. Engl.* **1982**, *21*, 209. (m) Chassot, L.; von Zelewsky, A. *Helv. Chim. Acta* **1986**, *69*, 1855. (n) Miskowski, V. M.; Houlding, V. H.; Che, C. M.; Wang, Y. *Inorg. Chem.* **1993**, *32*, 2518. (o) Zuleta, J. A.; Bevilacqua, J. M.; Eisenberg, R. *Coord. Chem. Rev.* **1991**, *111*, 237. (p) Zuleta, J. A.; Bevilacqua, J. M.; Proserpio, D. M.; Harvey, P. D.; Eisenberg, R. *Inorg. Chem.* **1992**, *31*, 2396. (q) Houlding, V. H.; Miskowski, V. M. *Coord. Chem. Rev.* **1991**, *111*, 145. (r) Cornioley-Deuschel, C.; von Zelewsky, A. *Inorg. Chem.* **1987**, *26*, 3354. (s) Maestri, M.; Sandrini, D.; Balzani, V.; von Zelewsky, A.; Deuschel-Cornioley, C.; Joliet, P. *Helv. Chim. Acta* **1988**, *71*, 1053. (t) von Zelewsky, A.; Belser, P.; Hayoz, P.; Dux, R.; Husa, X.; Suckling, A.; Stoeckli-Evans, H. *Coord. Chem. Rev.* **1994**, *132*, 75. (u) Chan, C.-W.; Cheng, L.-K.; Che, C.-M. *Coord. Chem. Rev.* **1994**, *132*, 87. (v) Bevilacqua, J. M.; Eisenberg, R. *Inorg. Chem.* **1994**, *33*, 1886.

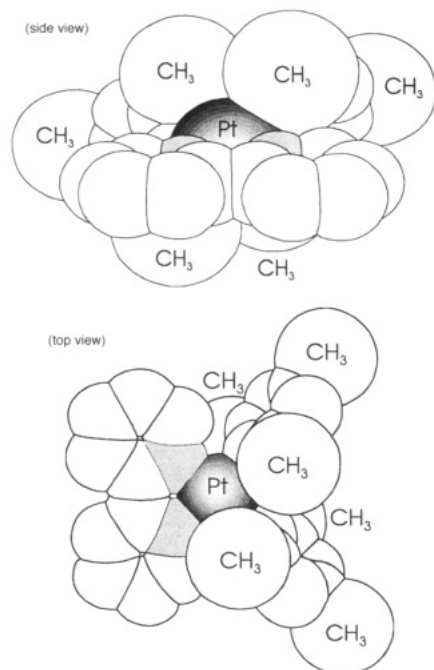
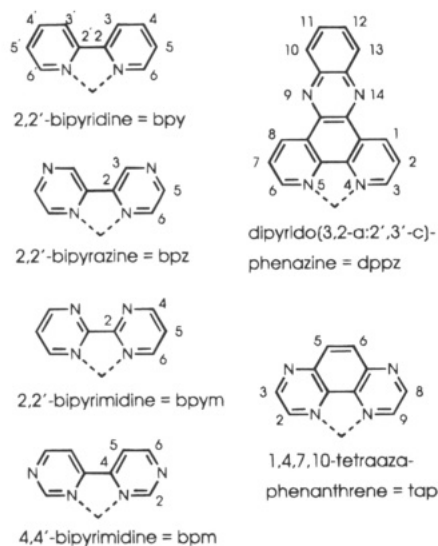


**Figure 1.** Space-filling model representations of the molecular structure of (bpy)PtMes<sub>2</sub>.

higher coordination numbers than four, approaching the low-spin d<sup>6</sup> situation with its extreme preference for hexacoordination.

In this paper we describe the consequences of axial shielding of essentially square planar coordinated platinum in mononuclear complexes (N<sup>∧</sup>N)Pt(Mes)<sub>2</sub> where Mes is mesityl (2,4,6-trimethylphenyl) and N<sup>∧</sup>N are α-diimine ligands of the 2,2'-bipyridine type.



In a recent structural study<sup>6</sup> of (bpy)PtMes<sub>2</sub>, the first mesitylplatinum compound to be characterized,<sup>7</sup> we pointed out that two such axially protecting aryl ligands can block the access of molecules to these open coordination sites, thereby preventing one of the most typical reactions of Pt(II) compounds, viz., oxidative addition by alkyl halides.<sup>2</sup> Figure 1 illustrates the structural

(6) Klein, A.; Hausen, H.-D.; Kaim, W. *J. Organomet. Chem.* **1992**, *440*, 207.

(7) For a later report of a structurally characterized mesitylplatinum(II) compound, see: Fallis, K. A.; Anderson, G. K.; Rath, N. P. *Organometallics* **1993**, *12*, 2435.

situation of (bpy)PtMes<sub>2</sub> using a space-filling model.

Results from cyclic voltammetry and EPR as well as UV/Vis/near-IR spectroelectrochemistry (one-electron oxidation, two one-electron reductions) are being presented now for various complexes (N<sup>∧</sup>N)PtMes<sub>2</sub> and for the related species (bpy)PtClMes and (bpy)Pt(o-CF<sub>3</sub>-Ph)<sub>2</sub>. There have been some recent studies of singly reduced Pt(II) complexes with heterocyclic anion radical ligands,<sup>2e,6,8</sup> on the other hand, the number of persistent mononuclear Pt(III) species is still rather small<sup>9,10</sup> although such states have been discussed as intermediates.<sup>11</sup> There are of course several stable oligonuclear species formally involving Pt(III).<sup>12</sup> Room-temperature absorption and emission spectra of the neutral Pt(II) complexes will also be reported here, including the effects of different solvents (solvatochromism).<sup>2e,50</sup>

## Experimental Section

**Materials.** The ligands bpm<sup>13</sup> and dppz,<sup>14</sup> which are not commercially available, and the platinum precursor complexes (DMSO)<sub>2</sub>PtMes<sub>2</sub> and (DMSO)<sub>2</sub>Pt(o-CF<sub>3</sub>Ph)<sub>2</sub><sup>15</sup> were obtained following literature procedures. Although the solid Pt(II) complexes are air-stable, their preparation and investigation was carried out under argon in dried solvents.

**General Synthetic Procedure for Complexes (N<sup>∧</sup>N)-PtMes<sub>2</sub>.** In a typical reaction, 150 mg (0.225 mmol) of bis-(dimethylsulfoxido)dimesitylplatinum(II) was suspended together with 0.26 mmol of the corresponding α-diimine ligand in 40 mL of toluene and heated under reflux for ~3 days; less basic ligands N<sup>∧</sup>N required longer reaction times. The course of the reaction could be monitored via the disappearance of the sulfoxide vibration ν(S=O) at 1130 cm<sup>-1</sup>.<sup>16</sup> The products that precipitated on cooling to 4 °C were collected, washed with *n*-hexane, and treated with 1,2-dichloroethane. After filtration through a microporous frit to remove colloidal platinum, the

(8) (a) Braterman, P. S.; Song, J.-I.; Vogler, C.; Kaim, W. *Inorg. Chem.* **1992**, *31*, 222. (b) Braterman, P. S.; Song, J. I.; Wimmer, F. M.; Wimmer, S.; Kaim, W.; Klein, A.; Peacock, R. D. *Inorg. Chem.* **1992**, *31*, 5084. (c) MacGregor, S. A.; McInnes, E.; Sorbie, R. J.; Yellowlees, L. J. In *Molecular Electrochemistry of Inorganic, Bioinorganic and Organometallic Compounds*; Pombeiro, A. J. L., McCleverty, J. A., Eds.; Kluwer Academic Publishers: Dordrecht, The Netherlands, 1993; p 503.

(9) (a) Uson, R.; Fornies, J.; Tomas, M.; Menjon, B.; Bau, R.; Sünkel, K.; Kuwabara, E. *Organometallics* **1986**, *5*, 1576. (b) Uson, R.; Fornies, J.; Tomas, M.; Ara, I.; Menjon, B. *J. Organomet. Chem.* **1987**, *226*, 129. (c) Blake, A. J.; Gould, R. O.; Holder, A. J.; Hyde, T. I.; Lavery, A. J.; Odulate, M. O.; Schröder, M. *J. Chem. Soc., Chem. Commun.* **1987**, 118. (d) Blake, A. J.; Holder, A. J.; Hyde, T. I.; Schröder, M. *J. Chem. Soc., Chem. Commun.* **1987**, 987. (e) Pandey, K. K. *Coord. Chem. Rev.* **1992**, *121*, 1.

(10) Matrix-stabilized Pt(III) transients: (a) Geoffroy, M.; Bernardinelli, G.; Castan, P.; Chermette, H.; Deguenon, D.; Nour, S.; Weber, J.; Wermeille, M. *Inorg. Chem.* **1992**, *31*, 5056. (b) Wermeille, M.; Geoffroy, M.; Arrizabalaga, P.; Bernardinelli, G. *Inorg. Chim. Acta* **1993**, *211*, 81. (c) Waltz, W. L.; Lilie, J.; Walters, R. T.; Woods, R. J. *Inorg. Chem.* **1980**, *19*, 3284. (d) Boucher, H. A.; Lawrance, G. A.; Lay, P. A.; Sargeson, A. M.; Bond, A. M.; Sangster, D. F.; Sullivan, J. C. *J. Am. Chem. Soc.* **1983**, *105*, 4652.

(11) (a) Halpern, J.; Pribanic, M. *J. Am. Chem. Soc.* **1968**, *90*, 5942. (b) Glennon, C. S.; Hand, T. D.; Sykes, A. G. *J. Chem. Soc., Dalton Trans.* **1980**, 19.

(12) (a) Hollis, L. S.; Lippard, S. J. *J. Am. Chem. Soc.* **1981**, *103*, 6761. (b) Renn, O.; Albinati, A.; Lippert, B. *Angew. Chem.* **1990**, *102*, 71; *Angew. Chem., Int. Ed. Engl.* **1990**, *29*, 84. (c) Matsumoto, K.; Sakai, K.; Nishio, K.; Tokisue, Y.; Ito, R.; Nishide, T.; Shichi, Y. *J. Am. Chem. Soc.* **1992**, *114*, 8110. (d) Baxter, L. A. M.; Heath, G. A.; Raptis, R. G.; Willis, A. C. *J. Am. Chem. Soc.* **1992**, *114*, 6944. (e) Uson, R.; Fornies, J.; Tomas, M.; Casas, J. M.; Cotton, F. A.; Falvello, L. R.; Feng, X. *J. Am. Chem. Soc.* **1993**, *115*, 4145.

(13) Effenberger, F. *Chem. Ber.* **1965**, *98*, 2260.

(14) Amouyal, E.; Homsy, A.; Chambron, J. C.; Sauvage, J. P. *J. Chem. Soc., Dalton Trans.* **1990**, 1841.

(15) Eaborn, C.; Kundu, K.; Pidcock, A. J. *J. Chem. Soc., Dalton Trans.* **1981**, 933.

(16) Cotton, F. A.; Francis, R.; Horrocks, W. D. Jr., *J. Phys. Chem.* **1960**, *64*, 1534.

dissolved complex was precipitated by dropwise addition of *n*-hexane and dried *in vacuo*. Typical yields were 85%; the yellow to dark-red compounds gave satisfactory analyses (C, H, N; available as supplementary material).

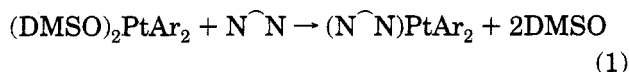
**(bpy)PtClMes.** In analogy to a published procedure,<sup>17</sup> a solution of 9.5 mg (0.12 mmol) of acetyl chloride in 10 mL of toluene was slowly added to a suspension of 60 mg (0.1 mmol) of (bpy)PtMes<sub>2</sub><sup>6</sup> in 30 mL of toluene/ethanol (5/1). After ~1 h the color change from red to yellow indicated the completion of the reaction. Removal of the solvent, washing with pentane, and drying under vacuum yielded 43 mg (85%) of the yellow compound. Analysis (C, H, N). <sup>1</sup>H NMR ((CD<sub>3</sub>)<sub>2</sub>SO): δ 9.33 (d, 1H, H<sub>6</sub>), 8.62 (d, 1H, H<sub>3</sub>), 8.56 (d, 1H, H<sub>3'</sub>), 8.38 (t, 1H, H<sub>4</sub>), 8.32 (t, 1H, H<sub>4'</sub>), 8.08 (d, 1H, H<sub>6'</sub>), 7.93 (t, 1H, H<sub>5</sub>), 7.52 (t, 1H, H<sub>5'</sub>), 6.59 (s, 2H, H<sub>Mes</sub>), 2.29 (s, 3H, *p*-CH<sub>3</sub>), 2.20 (s, 6H, *o*-CH<sub>3</sub>). UV/Vis (λ<sub>max</sub>): 465, 436, 407, 388, 362 nm (toluene); 450 sh, 422, 379, 353 nm (THF). The compound could also be obtained by using hydrochloric acid and stopping the reaction after ~30 min; longer reaction times produced (bpy)PtCl<sub>2</sub>.<sup>18</sup>

**(bpy)Pt(*o*-CF<sub>3</sub>Ph)<sub>2</sub>.** A suspension of 164 mg (0.255 mmol) of (DMSO)<sub>2</sub>Pt(*o*-CF<sub>3</sub>Ph)<sub>2</sub> and 41 mg (0.26 mmol) of 2,2'-bipyridine in 40 mL of toluene was heated under reflux for 2 days. After cooling to 4 °C for 24 h, the yellow precipitate was collected by filtration, washed with hexane, and recrystallized several times from 1,2-dichloroethane/heptane (1/3) to yield 133 mg (81%) of yellow microcrystals. Analysis (C, H, N). <sup>1</sup>H NMR (Table 1). UV/Vis (λ<sub>max</sub>): 441 sh, 436, 420, 365 nm (toluene).

**Instrumentation.** EPR spectra were recorded in the X band on a Bruker System ESP 300 equipped with a Bruker ER035M gaussmeter and a HP 5350B microwave counter. <sup>1</sup>H-NMR spectra were taken on a Bruker AC 250 spectrometer, infrared spectra were obtained using Perkin-Elmer 684 and 283 instruments. UV/Vis/near-absorption spectra were recorded on Shimadzu UV160 and Bruins Instruments Omega 10 spectrophotometers. A Perkin-Elmer fluorescence spectrometer LS-3B served to record emission spectra. Cyclic voltammetry and differential pulse voltammetry were carried out in THF, 1,2-dichloroethane, or acetonitrile/0.1 M Bu<sub>4</sub>NPF<sub>6</sub>, using a three-electrode configuration (glassy carbon electrode, Pt counter electrode, Ag/AgCl reference) and a PAR 273 potentiostat and function generator. The ferrocene/ferrocenium couple served as internal reference. Spectroelectrochemical measurements were performed using an optically transparent thin-layer electrode (Ottle) cell<sup>19</sup> for UV/Vis spectra and a two-electrode capillary for EPR studies.<sup>20</sup>

## Results

Due to the steric requirements of two mesityl groups and the general sluggishness of substitution reactions at Pt(II) the formation (eq 1) of the complexes (N<sup>∞</sup>N)-



PtMes<sub>2</sub> required long reaction times at elevated temperatures with the eventual formation of some decomposition products such as elemental platinum. The use of (DMSO)PtMes<sub>2</sub> gave the best results in terms of purity and yield. Nevertheless, reactions with the weakly basic ligand bpm<sup>21</sup> required longer times, and N=N function-containing ligands such as 3,3'-bipy-

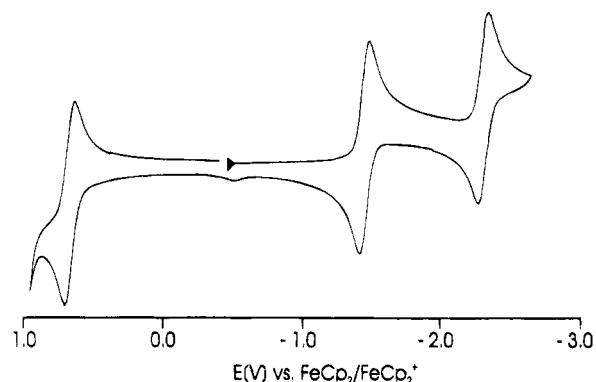


**Figure 2.** Cyclic voltammogram of (tap)PtMes<sub>2</sub> in THF/0.1 M Bu<sub>4</sub>NPF<sub>6</sub> at 100 mV/s scan rate.

ridazine<sup>21</sup> or 2,2'-azobispyridine<sup>22</sup> failed to show any significant conversion to the corresponding compounds (N<sup>∞</sup>N)PtMes<sub>2</sub> although the analogous dichloroplatinum(II) complexes could be obtained.<sup>23a</sup> The use of 3,6-bis(2-pyridyl)-1,2,4,5-tetrazine<sup>22</sup> and longer reaction times in the case of N<sup>∞</sup>N = 2,2'-bipyrimidine produced little soluble dinuclear complexes, which will be described separately.<sup>23b</sup> Brief (<30 min) action of hydrochloric acid on (bpy)PtMes<sub>2</sub> gave the mixed product (bpy)PtClMes, which could also be synthesized in a more controlled fashion by the action of acetyl chloride in a protic solvent mixture; (bpy)PtCl<sub>2</sub> is the reaction product after longer reaction times. The DMSO substitution method (eq 1) was also employed to prepare (bpy)Pt(*o*-CF<sub>3</sub>Ph)<sub>2</sub>, which was desired in order to evaluate the steric shielding of the *o*-(trifluoromethyl)phenyl substituent and to test the suitability of carbon-bonded fluoride atoms for protection of cationic Pt(III).

The complexes were identified primarily by <sup>1</sup>H-NMR spectroscopy, which revealed solvent-dependent chemical shifts of the protons of the heterocyclic ligands and variable spin-spin coupling involving the <sup>195</sup>Pt nuclei (*I* = 1/2, 33.8%); Table 1 summarizes the relevant data.

The ability of complexes (N<sup>∞</sup>N)PtMes<sub>2</sub> to add or lose electrons was studied by cyclic voltammetry with very similar results in THF, acetonitrile, or 1,2-dichloroethane, Figure 2 shows a typical cyclovoltammogram, and Table 2 contains the electrochemical data.

All complexes (N<sup>∞</sup>N)PtMes<sub>2</sub> show a reversible one-electron reduction wave, a mostly reversible second one-electron reduction step, and one reversible oxidation wave with the same current, as determined by cyclic voltammetry, differential pulse voltammetry and coulometry. Whereas the first reduction and oxidation processes meet all reversibility criteria even at scan rates of 20 mV/s, the second reduction becomes fully reversible only at 1000 mV/s for some complexes, as indicated by the large peak potential differences in Table 2. The second oxidation is always irreversible as is the first oxidation of complexes (bpy)PtClMes, (bpy)Pt(*o*-CF<sub>3</sub>Ph)<sub>2</sub>, (bpy)PtCl<sub>2</sub>, and (DMSO)PtMes<sub>2</sub>.

The generally reversible first reduction processes allowed us to generate persistent anionic species for EPR and UV/Vis/near-IR spectroelectrochemistry. EPR spectra were recorded in fluid solution at room temperature and in the frozen state; Figure 3 shows typical

(17) Clark, H. C.; Manzer, L. E. *J. Organomet. Chem.* **1973**, *59*, 411.

(18) Morgan, G. T.; Burstall, F. H. *J. Chem. Soc.* **1954**, 965.

(19) Krejciak, M.; Danek, M.; Hartl, F. *J. Electroanal. Chem.* **1991**, *317*, 179.

(20) Kaim, W.; Ernst, S.; Kasack, V. *J. Am. Chem. Soc.* **1990**, *112*, 173.

(21) Ernst, S.; Kaim, W. *J. Am. Chem. Soc.* **1987**, *108*, 3578.

(22) Kaim, W.; Kohlmann, S. *Inorg. Chem.* **1987**, *26*, 68.

(23) (a) Klein, A. Ph.D. Thesis, Universität Stuttgart, 1994. (b) Klein, A.; Kaim, W. Manuscript in preparation.

Table 1.  $^1\text{H-NMR}$  Data<sup>a</sup> of Complexes ( $\text{N}^-\text{N}$ )PtAr<sub>2</sub>

complex	$\text{N}^-\text{N}$ ligand		PtAr <sub>2</sub> fragment	
	$\delta^a$	$J^b$	$\delta^a$	$J^b$
(bpy)PtMes <sub>2</sub>		In (CD <sub>3</sub> ) <sub>2</sub> SO		
	8.58 dd (3,3')	7.80 (H3, H4)	6.51 s <sup>c</sup> (HMes)	14.80 (Pt, HMes)
	8.31 dd (4,4')	7.30 (H4, H5)	2.34 s (oCH <sub>3</sub> )	
	8.14 dd (6,6')	5.57 (H5, H6)	2.10 s (pCH <sub>3</sub> )	
(bpm)PtMes <sub>2</sub>	7.61 dd (5,5')			
	9.48 d (5,5')	5.30 (H5, H6)	6.51 s <sup>c</sup> (HMes)	15.72 (Pt, HMes)
	8.79 dd <sup>c</sup> (6,6')	7.43 (Pt, H6)	2.36 s (oCH <sub>3</sub> )	
	8.71 d <sup>c</sup> (2,2')	13.60 (Pt, H2)	2.13 s (pCH <sub>3</sub> )	
(bpz)PtMes <sub>2</sub>	1.02 (H2, H6)			
	9.96 s (3,3')	<1.0 (H3, H5)	6.56 s <sup>c</sup> (HMes)	15.67 (Pt, HMes)
	8.96 d (6,6')	3.01 (H5, H6)	2.31 s (oCH <sub>3</sub> )	
(bpym)PtMes <sub>2</sub>	8.20 dd (5,5')		2.14 s (pCH <sub>3</sub> )	
	9.38 dd (6,6')	2.17 (H4, H6)	6.52 s <sup>c</sup> (HMes)	14.69 (Pt, HMes)
	8.33 dd (4,4')	5.56 (H4, H5)	2.35 s (oCH <sub>3</sub> )	
	7.86 dd (5,5')	4.74 (H5, H6)	2.11 s (pCH <sub>3</sub> )	
(tap)PtMes <sub>2</sub>	9.96 d (5,6)	1.10 (H2, H5)	6.57 s <sup>c</sup> (HMes)	14.47 (Pt, HMes)
	8.95 d (3,8)	3.04 (H2, H3)	2.31 s (oCH <sub>3</sub> )	22.00 (Pt, H2, H9)
	8.20 dd (2,9)		2.14 s (pCH <sub>3</sub> )	
(dppz)PtMes <sub>2</sub>	9.83 dd (1,8)	8.19 (H7, H8)	6.58 s (HMes)	
	8.57 dd (3,6)	5.22 (H6, H7)	2.43 s (oCH <sub>3</sub> )	
	8.47 dd (10,13)	6.58 (H10, H11)	2.16 s (pCH <sub>3</sub> )	
	8.14 dd (11,12)	3.41 (H10, H12)	8.12 dd (2,7)	1.42 (H6, H8)
(bpy)Pt(o-CF <sub>3</sub> Ph) <sub>2</sub>	8.65 d (3,3')	8.09 (H3, H4)	7.94 dd (6,6') <sup>d</sup>	
	8.34 dd (4,4')	7.65 (H4, H5)	7.80 t (3,3') <sup>d</sup>	
	7.62 dd (5,5')	5.55 (H5, H6)	7.13 t (5,5') <sup>d</sup>	
	7.45 dd (6,6')	1.94 (H4, H6)	7.01 m (4,4') <sup>d</sup>	
(bpm)PtMes <sub>2</sub>		In CD <sub>2</sub> Cl <sub>2</sub>		
	9.32 d (5,5')	5.23 (H5, H6)	6.67 s <sup>c</sup> (HMes)	15.74 (Pt, HMes)
	9.07 d <sup>c</sup> (2,2')	12.87 (Pt, H2,2')	2.42 s <sup>c</sup> (oCH <sub>3</sub> )	6.66 (Pt, oCH <sub>3</sub> )
	8.04 dd (6,6')	1.27 (H2, H6)	2.21 s (pCH <sub>3</sub> )	
(tap)PtMes <sub>2</sub>	9.47 dd (5,5')	1.30 (H2, H5)	6.69 s <sup>c</sup> (HMes)	15.33 (Pt, HMes)
	8.76 d <sup>c</sup> (3,8)	3.00 (H2, H3)	2.37 s <sup>c</sup> (oCH <sub>3</sub> )	5.99 (Pt, oCH <sub>3</sub> )
	8.48 dd (2,9)	20.62 (Pt, H2,9)	2.23 s (pCH <sub>3</sub> )	7.72 (Pt, H3,8)

<sup>a</sup> Chemical shifts  $\delta$  in ppm (positions in parentheses). <sup>b</sup> Coupling constants  $J$  in hertz (coupling nuclei in parentheses); HMes, meta protons; oCH<sub>3</sub>, ortho methyl groups; pCH<sub>3</sub>, para methyl groups of mesityl ligand. <sup>c</sup> <sup>195</sup>Pt isotope coupling ( $I = 1/2$ ; 33.8% natural abundance). <sup>d</sup> CF<sub>3</sub> substituent in position 2 (ortho position);  $J$  values not available due to insufficient resolution.

Table 2. Electrochemical Data<sup>a</sup> of Complexes ( $\text{N}^-\text{N}$ )PtAr<sub>2</sub> and Related Species

complex	$E_{\text{pa}}^{\text{oxII}}$	$E_{1/2}^{\text{oxI}}$	$E_{1/2}^{\text{redI}}$	$E_{1/2}^{\text{redII}}$
(bpy)PtMes <sub>2</sub> <sup>b</sup>	1.01	0.45 (60)	-2.05 (60)	-2.73 (80)
(bpm)PtMes <sub>2</sub> <sup>b</sup>	1.02	0.53 (60)	-1.37 (62)	-2.12 (78)
(bpz)PtMes <sub>2</sub> <sup>b</sup>	1.06	0.59 (62)	-1.47 (63)	-2.34 (135)
(bpym)PtMes <sub>2</sub> <sup>b</sup>	0.98	0.54 (63)	-1.67 (61)	-2.38 (102)
(tap)PtMes <sub>2</sub> <sup>b</sup>	1.05	0.60 (68)	-1.49 (65)	-2.35 (68)
(dppz)PtMes <sub>2</sub> <sup>b</sup>	1.00	0.49 (67)	-1.50 (62)	-2.24 (95)
(bpy)PtClMes <sup>c</sup>	1.19	0.83 (irr) <sup>d</sup>	-1.80 (69)	-2.47 (114)
(bpy)Pt(o-CF <sub>3</sub> Ph) <sub>2</sub> <sup>c</sup>		0.91 (irr) <sup>d</sup>	-1.86 (66)	-2.56 (91)
(bpy)PtPh <sub>2</sub> <sup>c</sup>		0.52 (irr) <sup>d</sup>	-2.08 (60)	-2.75 (83)
(bpy)PtCl <sub>2</sub> <sup>b</sup>	1.19	0.67 (irr) <sup>d</sup>	-1.64 (83)	-2.30 (84)
(DMSO) <sub>2</sub> PtMes <sub>2</sub> <sup>b</sup>	1.18	0.89 (irr) <sup>d</sup>		

<sup>a</sup> From cyclic voltammetry in 0.1 M Bu<sub>4</sub>NPF<sub>6</sub> solutions at 100 mV/s scan rate. Potentials  $E_{1/2}$  (in V) vs FeCp<sub>2</sub><sup>0/+</sup>, peak potential differences (in mV) in parentheses. Anodic peak potentials  $E_{\text{pa}}$  for the second oxidation step (oxII). <sup>b</sup> In THF. <sup>c</sup> In acetonitrile. <sup>d</sup> Anodic peak potential  $E_{\text{pa}}$ .

spectra and Table 3 contains a summary of pertinent data. The rather high line width and the significant deviations of isotropic  $g$  factors,  $g_{\text{iso}}$ , from the free electron value of 2.0023 are not unexpected for radial complexes of a 5d element; furthermore, the frequently observed isotropic <sup>195</sup>Pt satellite splitting,  $a_{\text{iso}}(^{195}\text{Pt})$ , allowed us to obtain a corresponding correlation between  $g_{\text{iso}}$  and  $a_{\text{iso}}$  (Figure 4).

All attempts to observe EPR spectra of electrogenerated cations failed. These attempts included *intra muros* electrolysis at 293 K as well as brief (1 min) *extra muros* electrolyses at room temperature or slightly longer low-temperature electrolyses (at 240 K) and then rapid freezing to a glassy solution at 77 K. EPR

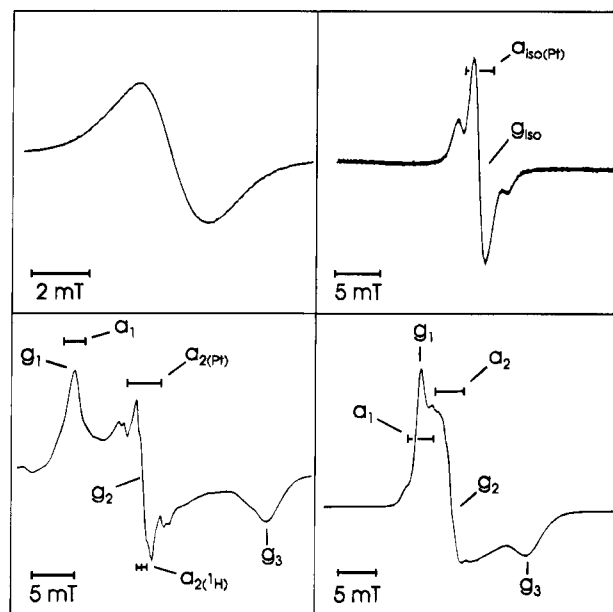


Figure 3. EPR spectra of [(tap)PtMes<sub>2</sub>]<sup>-</sup> (left) and [(bpym)PtMes<sub>2</sub>]<sup>-</sup> (right), electrogenerated in THF/0.1 M Bu<sub>4</sub>NPF<sub>6</sub>, in fluid solution at 293 K (top) and in glassy frozen solution at 150 K (bottom).

measurements of all thus generated complexes [( $\text{N}^-\text{N}$ )PtMes<sub>2</sub>]<sup>-</sup> between 4 and 300 K failed to exhibit any signals for Pt(III) centers.

Absorption and emission spectra of the complexes were recorded at room temperature in solution. Figure

Table 3. EPR Data<sup>a</sup> of Anion Radical Complexes<sup>b</sup> [(N<sup>−</sup>N)PtAr<sub>2</sub>]<sup>−</sup>

radical complex	$g_{\text{iso}}(293\text{K})$	$g$ components			$\Delta g^c$	$a(\text{Pt})_{\text{iso}}$	$a(\text{Pt})$ components			further hyperfine splitting
		$g_1$	$g_2$	$g_3$			$a_1$	$a_2$	$a_3$	
[(bpy)PtMes <sub>2</sub> ] <sup>−</sup>	1.9898	2.0312	2.0071	1.9340 <sup>d</sup>	972	4.0	5.2	3.8	<3.4 <sup>d</sup>	
[(bpm)PtMes <sub>2</sub> ] <sup>−e</sup>	1.9972	2.0302	2.0054	1.954 <sup>f</sup>	762	<1.7	<1.6	2.2	<2.5 <sup>f</sup>	
[(bpz)PtMes <sub>2</sub> ] <sup>−</sup>	1.9964	2.0573	2.0056	1.9200 <sup>d</sup>	1373	2.8	3.5	nd <sup>l</sup>	<2.1 <sup>d</sup>	0.53 <sup>i</sup>
[(bpym)PtMes <sub>2</sub> ] <sup>−</sup>	1.9927	2.0291	2.0051	1.9453 <sup>d</sup>	838	3.0	3.6	~3.0	<2.5 <sup>d</sup>	
[(tap)PtMes <sub>2</sub> ] <sup>−</sup>	1.9964	2.0579	2.0058	1.9213 <sup>d</sup>	1366	<2.4	2.5	4.1	<2.5 <sup>d</sup>	0.62 <sup>j</sup>
[(dppz)PtMes <sub>2</sub> ] <sup>−</sup>	2.0035	2.0069	2.0039	2.0039 <sup>g</sup>	30	<0.2	nd	g		0.52 <sup>k</sup>
[(bpy)Pt( <i>o</i> -CF <sub>3</sub> Ph) <sub>2</sub> ] <sup>−</sup>	1.9937	2.0236	2.0065	1.9502 <sup>g</sup>	734	2.1	2.6	2.8	<2.5 <sup>g</sup>	
[(bpy)PtClMes] <sup>−e</sup>	1.9914	2.031	2.004	1.931 <sup>f</sup>	1000	4.7	3.0	4.5	<3.8 <sup>f</sup>	
[(bpy)PtCl <sub>2</sub> ] <sup>−h</sup>	1.9988	2.038	2.009	1.935 <sup>h</sup>	1030	5.8	5.9	10.1	2.5 <sup>h</sup>	

<sup>a</sup> Coupling constants for nuclei <sup>1</sup>H, <sup>14</sup>N, or <sup>195</sup>Pt ( $I = 1/2$ , 33.8% natural abundance) (in mT). Data from graphical spectra analysis (see Figure 3); errors estimated for  $a_1$ ,  $a_2$ , and  $a_3$  are  $\pm 0.3$  mT. <sup>b</sup> Generated from neutral precursors by cathodic reduction in 1,2-dichloroethane/0.1 M Bu<sub>4</sub>NPF<sub>6</sub> or Bu<sub>4</sub>NClO<sub>4</sub>. <sup>c</sup>  $\Delta g = (g_1 - g_3) \times 10^4$ . <sup>d</sup> At 150 K. <sup>e</sup> In THF/0.1 M Bu<sub>4</sub>NPF<sub>6</sub>. <sup>f</sup> At 110 K. <sup>g</sup> At 120 K. <sup>h</sup> At 77 K in DMF/0.1 M Bu<sub>4</sub>NBF<sub>4</sub>, from ref 8c. <sup>i</sup> Triplet coupling (H5,5') at 150 K. <sup>j</sup> Triplet coupling (Figure 3)  $a_2(\text{H3}, 8)$ , at 150 K. <sup>k</sup> Quintet coupling (N9,14), at 293 K. <sup>l</sup> nd, not detected.

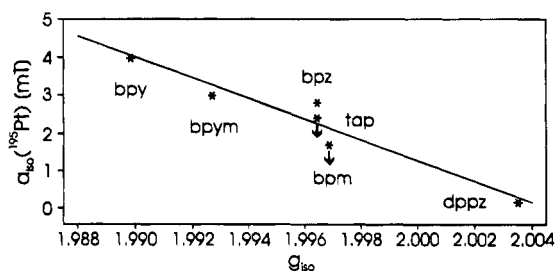


Figure 4. Correlation of isotropic  $g$  factors  $g_{\text{iso}}$  with isotropic hyperfine coupling constants  $a_{\text{iso}}(^{195}\text{Pt})$  of radical complexes [(N<sup>−</sup>N)PtMes<sub>2</sub>]<sup>−</sup> (↓, upper limit). Least-squares fit:  $a_{\text{iso}} = 543.096 \text{ mT} - (g_{\text{iso}} \cdot 270.915 \text{ mT})$ ;  $r = 0.969$  (correlation coefficient).

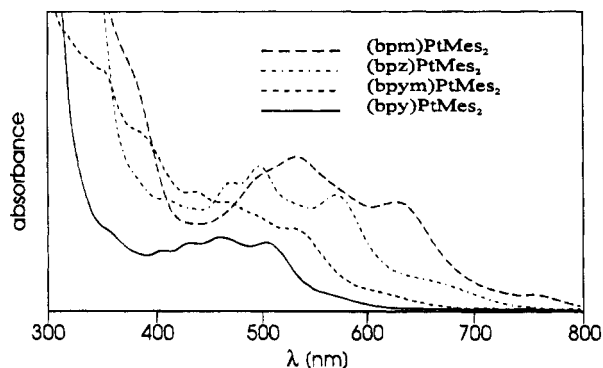


Figure 5. Absorption spectra of complexes (N<sup>−</sup>N)PtMes<sub>2</sub> in toluene. Intensities different for each spectrum.

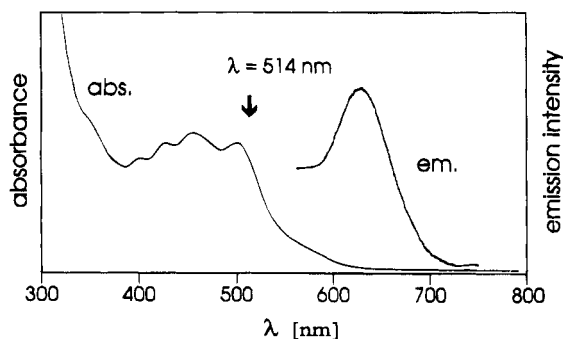


Figure 6. Emission spectrum of (bpy)PtMes<sub>2</sub> at 293 K in toluene solution; excitation wavelength 514 nm.

Figure 5 contains representative absorption spectra; Figure 6 illustrates the absorption and emission spectrum of the bpy complex. Absorption and emission maxima are summarized in Tables 4 and 5.

The absorption maxima of the complexes exhibit the typical<sup>2e,5o,24-26</sup> negative solvatochromism, i.e., a high-

Table 4. Absorption Maxima<sup>a</sup> of Complexes (N<sup>−</sup>N)PtMes<sub>2</sub> in Toluene

N <sup>−</sup> N	$\lambda_{\text{max}}$		
	<sup>3</sup> MLCT <sup>b</sup>	<sup>1</sup> MLCT	
bpy	570 (sh);	504, 459, 432, 406;	352 (sh)
bpm	760;	631, 535, 503 (sh);	372 (sh)
bpz	650 (sh);	573, 499, 483;	406
bpym	610 (sh);	529, 494sh, 472, 430;	382 (sh), 352 (sh)
tap	660 (sh);	567, 498, 470, 408 (sh)	
dppz	570 (sh);	500 sh, 436 (sh);	378, 362, 345

<sup>a</sup> Wavelengths  $\lambda$  in nanometers. Most intense band within a group italic. <sup>b</sup> Weak bands.

Table 5. Long-Wavelength Emission and Absorption Data<sup>a</sup> for Complexes (N<sup>−</sup>N)PtAr<sub>2</sub>

complex	emission (excitation)			absorption $\tilde{\nu}_{\text{max}}^{\text{abs}}$	Stokes shift $\Delta^a$
	$\lambda_{\text{max}}^{\text{em}}$	$\tilde{\nu}_{\text{max}}^{\text{em}}$	$\lambda_{\text{ex}}$		
(bpy)PtMes <sub>2</sub>	610	16 390 (506)		19 840	3450
(bpz)PtMes <sub>2</sub>	590 sh	16 959 (470)		17 640	690
(bpym)PtMes <sub>2</sub>	591	16 920 (500)		18 900	1980
(tap)PtMes <sub>2</sub>	580	17 240 (488)		17 640	400
(dppz)PtMes <sub>2</sub>	592	16 890 (514)		19 490	2600
(bpy)Pt( <i>o</i> -CF <sub>3</sub> Ph) <sub>2</sub>	508	19 680 (430)		22 670	3000
(bpy)PtClMes	558	17 920 (470)		21 500	3580

<sup>a</sup> From measurements in toluene at 293 K. Wavelengths in nanometers; wavenumbers and Stokes shifts  $\Delta = \tilde{\nu}_{\text{max}}^{\text{abs}} - \tilde{\nu}_{\text{max}}^{\text{em}}$  in reciprocal centimeters. No emission was observed for (bpm)PtMes<sub>2</sub>.

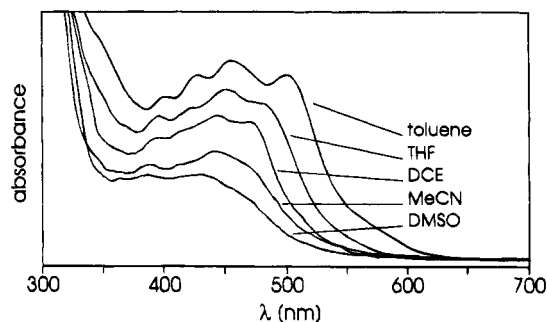


Figure 7. Solvatochromism of (bpy)PtMes<sub>2</sub> in different solvents at room temperature (DCE = 1,2-dichloroethane). Intensities different for each spectrum.

energy shift in more "polar" solvents (Figure 7, Table 6). Table 6 summarizes the solvent dependence for the long-wavelength absorption features; higher energy MLCT absorption components, e.g., of (bpy)PtMes<sub>2</sub>, show a similar extent of the negative solvatochromic

(24) Kaim, W.; Kohlmann, S.; Ernst, S.; Olbrich-Deussner, B.; Bessenbacher, C.; Schulz, A. *J. Organomet. Chem.* **1987**, *321*, 215.

(25) Manuta, D. M.; Lees, A. *J. Inorg. Chem.* **1983**, *22*, 3825.

(26) Reichardt, C. *Solvents and Solvent Effects in Organic Chemistry*, 2nd ed.; VCH: Weinheim, Germany, 1988.

Table 6. Solvent Dependence of Long-Wavelength Absorption Maxima  $\bar{\nu}_{\max}$  of Complexes  $(\widehat{N}N)\text{PtMes}_2$ 

$(\widehat{N}N)$	$\bar{\nu}_{\max}$ [ $\text{cm}^{-1}$ ]				correlation parameters <sup>a</sup>		
	toluene	THF	MeCN	DMSO	A ( $\text{cm}^{-1}$ )	B ( $\text{cm}^{-1}$ )	r
bpy	19 840	20 830	21 505 (sh) <sup>a</sup>	21 840 (sh) <sup>a</sup>	19 180	2670	0.966
bpm	15 850	17 330	17 920	18 250 (sh)	14 880	3440	0.997
bpz	17 450	18 620	19 120	19 420	16 790	2680	0.979
bpym	18 900	20 370	20 700 (sh)	20 920 (sh)	17 700	3125	0.984
tap	17 640	18 620 (sh)	19 420	19 380 (sh)	16 870	2730	0.986
dppz	19 490	20 280 (sh)	21 510	21 640 (sh)	18 480	3230	0.995

<sup>a</sup> Linear regression  $\bar{\nu}_{\max} = A + BE^*_{\text{MLCT}}$ ; correlation coefficient r.  $E^*_{\text{MLCT}} = 0.30$  (toluene), 0.59 (THF), 0.90 (MeCN), and 1.00 (DMSO).

Table 7. Absorption Data<sup>a</sup> of Complexes  $[(\widehat{N}N)\text{PtMes}_2]^{\pm}$  in THF/0.1 M  $\text{Bu}_4\text{NPF}_6$ 

$\widehat{N}N$	$\lambda_{\max}$ ( $\epsilon \times 10^{-3}$ ) for $n = 0$ ; MLCT	$\lambda_{\max}$ ( $\epsilon \times 10^{-3}$ ) for $n = 1$				$\lambda_{\max}$ for $n = 2$ ; IL		
		IL1		IL2			IL3	IL4
bpy	480 (2.46), 441 (2.69), 418 (sh), 393	1356 (0.2), 1120 (sh), 942 (1.2);		832 (1.3), 744 (1.0);		530 (5.2), 494 (4.9), 473 (sh);	371 (10.8)	529 (br), 397
bpm	577 (1.70), 487 (2.38)	737 (1.9), 666 (2.7);		603 (2.7), 551 (3.5);		492 (10.0), 461 (8.0), 440 (sh);	337 (12.0)	358 (br)
bpz	537 (2.58), 517 (sh), 480 (2.82), 458	1199 (2.9), 1077 (sh), 1027 (3.2);		526 (sh);		502 (6.0), 466 (5.0);	327 (sh)	500 (sh), 368
bpym	491 (1.50), 423 (sh)	1150 (sh), 950 (0.5), 828 (0.4);				506 (6.1), 477 (5.9), 453 (sh);	356 (sh)	377
tap	537 (sh), 532, 483, 457	1202, 1085 (sh), 1027;		523 (sh);		502, 466;	333 (sh)	
dppz	493 (sh), 423 (sh)	1345, 1208;				588, 558 (sh), 452;	342	825, 726, 453

<sup>a</sup> Wavelengths  $\lambda$  (in nm); molar extinction coefficients (in  $\text{M}^{-1} \text{cm}^{-1}$ ). MLCT, Metal-to-ligand charge transfer bands; IL, intraligand bands.

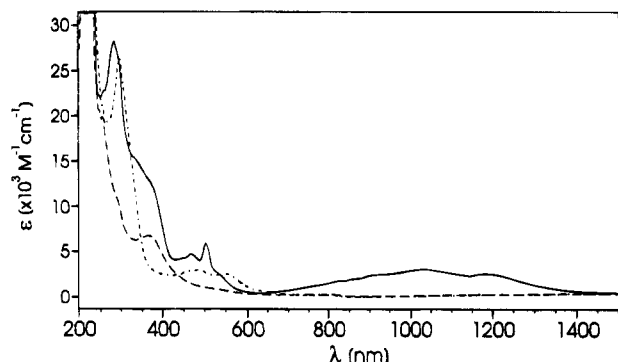


Figure 8. UV/Vis/near-IR absorption spectra from reductive spectroelectrochemistry of  $(\text{bpz})\text{PtMes}_2$  in THF/0.1 M  $\text{Bu}_4\text{NPF}_6$ : neutral complex (---); monoanion (—); dianion (-.-).

effect. Table 6 also contains parameters of the linear correlation with the best suitable solvent parameter,  $E^*_{\text{MLCT}}$ , which had been empirically derived from MLCT transitions of complexes  $(\text{bpy})\text{M}(\text{CO})_4$ ,  $\text{M} = \text{Mo}, \text{W}$ , by Manuta and Lees.<sup>25</sup> Attempts to obtain correlations with  $E_{\text{T}}$ ,  $\epsilon_{\text{r}}$ ,<sup>26</sup> or  $E_{\text{CT}}(\pi)$ <sup>27</sup> were less successful.

While the MLCT absorption maxima of the complexes  $(\widehat{N}N)\text{PtMes}_2$  exhibit negative solvatochromism (Table 6), the emission maxima show the opposite behavior, as noted here for  $(\text{bpy})\text{PtMes}_2$ :  $\nu_{\max}^{\text{em}} 16\,390$  (powder or toluene solution), 15 080 (1,2-dichloroethane), 14 140  $\text{cm}^{-1}$  (MeCN solution). Both effects are characteristic of a low-lying MLCT excited and emissive state.<sup>28</sup>

UV/Vis/near-IR spectroelectrochemical data were obtained for both the monoanions and the monocations. Figures 8 and 9 show typical such spectra; Tables 7 and 8 contain the pertinent data.

While the monoanions show the expected<sup>8,29,30</sup>

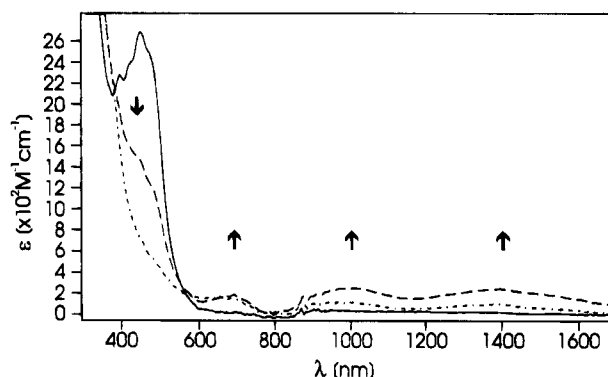


Figure 9. UV/Vis/near-IR absorption spectra from oxidative spectroelectrochemistry of  $(\text{bpy})\text{PtMes}_2$  in THF/0.1 M  $\text{Bu}_4\text{NPF}_6$ : neutral complex (—); monocation after 2 min (---); partially decomposed monocation after 4 min (-.-.-).

Table 8. Ligand-Field Absorption Maxima<sup>a</sup> of Spectroelectrochemically Generated Complexes  $[(\widehat{N}N)\text{PtMes}_2]^{\pm}$ 

$\widehat{N}N$	$\lambda_1$	$\bar{\nu}_1$	( $\epsilon$ )	$\lambda_2$	$\bar{\nu}_2$	( $\epsilon$ )	$\lambda_3$	$\bar{\nu}_3$	( $\epsilon$ )
bpy	687	14540	(257)	1001	9980	(316)	1394	7170	(320)
bpm	647	15450	(430)	956	10460	(474)	1387	7210	(618)
bpz	638	15660		948	10540		1376	7260	
bpz <sup>b</sup>	640	15610	(190)	944	10590	(275)	1408	7100	(480)
bpym	670 (sh)	14920 (sh)	(180)	970	10310	(135)	1440	6940	(208)
bpym <sup>b</sup>	671	14900		965	10360		1402	7130	
tap	721 (sh)	13860 (sh)		972	10290		1380	7240	
dppz	703	14220		969	10330		1404	7120	

<sup>a</sup> In THF/0.1 M  $\text{Bu}_4\text{NPF}_6$ , except where noted. Wavelengths  $\lambda$  (in nm); wavenumbers  $\bar{\nu}$  (in  $\text{cm}^{-1}$ ); molar extinction coefficients  $\epsilon$  (in  $\text{M}^{-1} \text{cm}^{-1}$ ).

<sup>b</sup> In 1,2-dichloroethane/0.1 M  $\text{Bu}_4\text{NPF}_6$ .

features of the individual ligand radical anions,  $(\widehat{N}N)^{\cdot-}$ , all monocations are distinguished by three weak bands at long wavelengths (600–1500 nm, Table 8). The typically slow electrolysis time in an Otte cell showed that the monoanions are generally stable under those conditions whereas the cations undergo a degradation reaction within minutes (Figure 9), despite the fully reversible redox process in the more rapid cyclic voltammetry experiment.

(27) Kaim, W.; Olbrich-Deussner, B.; Roth, T. *Organometallics* **1991**, *10*, 410.

(28) Zulu, M. M.; Lees, A. J. *Inorg. Chem.* **1988**, *27*, 3325.

(29) Krejčík, M.; Zalis, S.; Ladwig, M.; Matheis, W.; Kaim, W. *J. Chem. Soc., Perkin Trans. 2* **1992**, 2007.

(30) Fees, J.; Kaim, W.; Moscherosch, M.; Matheis, W.; Klima, J.; Krejčík, M.; Zalis, S. *Inorg. Chem.* **1993**, *32*, 166.

## Discussion

### Reactivity and Stability of Oxidation States.

The consequences of an apparently efficient axial protection of the platinum(II) center in complexes ( $\widehat{N\ N}$ )PtMes<sub>2</sub> (Figure 1) can be summarized as follows. First, the mere synthesis of these species requires fairly long reaction times due to the sterically hindered substitution reaction of (DMSO)<sub>2</sub>PtMes<sub>2</sub> (eq 1). As shown quantitatively in a previous report on oxidative addition behavior,<sup>2e</sup> the ligand basicity can be correlated with the reaction rate; similarly, the comparatively electron-rich bpy ligand substitutes for DMSO within 3 days whereas the weakly basic<sup>21</sup> bpm requires at least 4 days under the same conditions.

Second, thermal<sup>1,2</sup> and photoinduced<sup>5r,s</sup> oxidative addition reactions are blocked. This is evident from the addition of the standard reagent iodomethane to the prototypical complex (bpy)PtMes<sub>2</sub>, which does not show any sign of conversion after more than 6 months at room temperature, with or without light.<sup>6,23a</sup> A similar result had been reported for (dppm)PtMes<sub>2</sub>, dppm = bis-(diphenylphosphino)methane.<sup>32</sup> While hydrochloric acid reacts to hydrolyze the Pt–C bonds, it does so rather slowly with the formation of (bpy)PtClMes as isolable intermediate. Acetyl chloride does not react with, e.g., (bpy)PtMes<sub>2</sub> in dry THF, CH<sub>2</sub>Cl<sub>2</sub>, or MeCN; however, the HCl produced after addition of ethanol leads to (bpy)PtClMes. In contrast to the species ( $\widehat{N\ N}$ )PtMes<sub>2</sub>, the complex (bpy)Pt(*o*-CF<sub>3</sub>Ph)<sub>2</sub> readily adds iodomethane, which already suggests a lesser degree of axial shielding in this compound. In summary, the dimesitylplatinum complexes appear sterically shielded against external attack in the axial position, except for attacks by the smallest of electrophiles, H<sup>+</sup>.

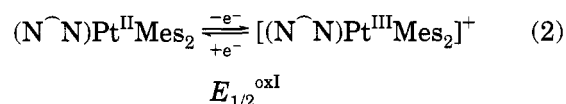
The most intriguing consequence of this axial shielding of the coordinatively unsaturated metal center by intramolecularly attached and seemingly inert mesityl substituents is the stabilization of the one-electron oxidized state, involving the rare<sup>9,10</sup> mononuclear Pt(III) center. This oxidation occurs at rather low potentials for all complexes ( $\widehat{N\ N}$ )PtMes<sub>2</sub> because of the electron-donating substituent effect from two mesityl groups; a smaller contribution from the varying donor capacity of the different heterocyclic ligands  $\widehat{N\ N}$  is also evident from Table 2. Axial protection by particularly bulky ligands should not only preclude any dimerization or other aggregation, more importantly, it should also prevent nucleophilic solvent molecules or electrolyte ions from attacking at the very reactive electrophilic metal center in the paramagnetic cations [( $\widehat{N\ N}$ )PtMes<sub>2</sub>]<sup>+</sup>. Previous studies on the irreversible oxidation of complexes ( $\widehat{N\ N}$ )PtPh<sub>2</sub> have shown a very pronounced solvent dependence of the anodic peak potential.<sup>2e</sup>

In fact, all dimesitylplatinum(II) complexes are oxidized in a clean, cyclovoltammetrically reversible one-electron step, as evident also from comparison (differential pulse voltammetry, coulometry) with the fully reversible one-electron reduction waves (Figure 2). However, the exchange of only one mesityl group by chloride as in (bpy)PtClMes makes the metal center

susceptible again to irreversible oxidation at a slightly higher potential (Table 2). It is thus evident that *both* mesityl substituents are necessary to provide the necessary axial protection (Figure 1) for stabilization of the Pt(III) state. Even so, the stability of that extremely reactive form is not high enough to obtain it as an isolable material. As the UV/Vis/near-IR spectroelectrochemical experiments show (Figure 9), the decay of electrogenerated Pt(III) cations proceeds within a few minutes at room temperature, thus permitting spectroscopic studies but not crystallization. Protection by one *o*-trifluoromethyl substituent instead of two *o*-methyl groups on each of the two aryl rings also proved detrimental to the stability of the Pt(III) form; irreversible anodic oxidation occurs for (bpy)Pt(*o*-CF<sub>3</sub>Ph)<sub>2</sub> at a relatively high potential (Table 2). In addition to a still insufficient axial protection against external attack, the possible intramolecular activation of the CH(methyl) bonds in mesityl substituents and the abstraction of fluoride in the case of (bpy)Pt(*o*-CF<sub>3</sub>Ph)<sub>2</sub> are conceivable causes for the decomposition of the Pt(III) species with their assumed reactive (5d<sub>z<sup>2</sup>-1</sub>)<sup>-1</sup> configuration. (The shortest nonbonded Pt–C(*o*-CH<sub>3</sub>) distance in (bpy)PtMes<sub>2</sub> is ~320 pm). Whereas the affinity of high oxidation state platinum for fluoride ligation is well established,<sup>33</sup> the oxidative addition of the C–H bond via an agostic intermediate to activated metal sites has recently been demonstrated in a number of cases.<sup>34,35</sup>

It should be noted here that the hitherto reported stable complexes of monomeric Pt(III) do not contain C–H bonds close to the metal center: The anion [Pt(C<sub>6</sub>Cl<sub>5</sub>)<sub>4</sub>]<sup>-</sup> contains no H at all,<sup>9a,b</sup> and the metal in [Pt(ttn)<sub>2</sub>]<sup>3+</sup><sup>9c,d</sup> is coordinated exclusively to the sulfur donor atoms of 1,4,7-trithiacyclononane (ttn).

After the fully reversible first oxidation to a Pt(III) cation (eq 2) which is persistent on the time scale (<1 min) of the cyclovoltammetry experiment, the second



oxidation wave is completely irreversible. It thus remains speculative whether this process is a straight Pt(III) → Pt(IV) transition or an oxidation involving the carbanionic aryl ligands.<sup>36</sup> As a d<sup>6</sup> center, Pt(IV) requires hexacoordination, which can be provided in sterically unhindered cases by solvent donor molecules such as MeCN or by halide ions.<sup>37</sup>

The stepwise reduction (eqs 3 and 4) of the complexes concerns primarily the heterocyclic acceptor ligands  $\widehat{N\ N}$ , the corresponding potentials thus show a variation and separation  $E_{1/2}^{\text{redI}} - E_{1/2}^{\text{redII}}$  that is typical for

(31) Shida, T. *Electronic Absorption Spectra of Radical Ions*; Elsevier Science Publishers: Amsterdam, 1988.

(32) Hassan, F. S. M.; McEwan, D. M.; Pringle, P. G.; Shaw, B. L. *J. Chem. Soc., Dalton Trans* **1985**, 1501.

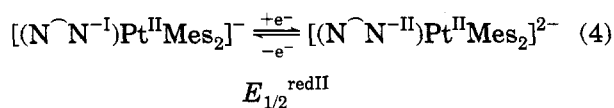
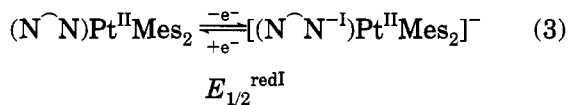
(33) (a) Anderson, C. M.; Crespo, M.; Ferguson, G.; Lough, A. J.; Puddephatt, R. J. *Organometallics* **1992**, *11*, 1177. (b) Crespo, M.; Martinez, M.; Sales, J. *J. Chem. Soc., Chem. Commun.* **1992**, 822.

(34) Crabtree, R. H.; Hamilton, D. G. *Adv. Organomet. Chem.* **1988**, *28*, 299.

(35) Ankaniec, B. C.; Hardy, D. T.; Thomson, S. K.; Watkins, W. N.; Young, G. B. *Organometallics* **1992**, *11*, 2591.

(36) (a) Kaim, W. *Top. Curr. Chem.* **1994**, *169*, 231. (b) Hasenzahl, S.; Kaim, W.; Stahl, T. *Inorg. Chim. Acta* **1994**, *225*, 23.

(37) (a) Davies, J. A.; Chen, L.; Eagle, C. T.; Staples, R. J. In *Molecular Electrochemistry of Inorganic, Bioinorganic and Organometallic Compounds*; Pombeiro, A. J. L., McCleverty, J. A., Eds.; Kluwer Academic Publishers: Dordrecht, The Netherlands, 1993; p 351. (b) Watzky, M. A.; Waknine, D.; Heeg, M. J.; Endicott, J. F.; Ochrymowycz, L. A. *Inorg. Chem.* **1993**, *32*, 4882.



the free ligands and their organometallic or other complexes.<sup>21,22,30,38</sup> The susceptibility for the reduction of  $(\widehat{N\ N})\text{PtMes}_2$  thus increases along the following sequence for  $\widehat{N\ N}$ : bpy < bpym < dppz  $\approx$  tap  $\approx$  bpz < bpm. In essence, this is also the sequence of increasing reducibility for the free ligands.<sup>21</sup>

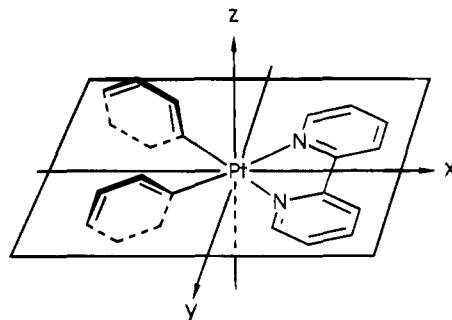
In comparison to  $\text{PtPh}_2$ , the  $\text{PtMes}_2$  complex fragment is a little less electrophilic and thus induces slightly more negative reduction potentials; the opposite is true for  $\text{Pt}(o\text{-CF}_3\text{Ph})_2$  and, of course, for  $\text{PtCl}_2$  (Table 2). A particular stabilization of the monoanions or dianions due to steric shielding could not be established; usually it is the small  $\text{H}^+$  electrophile that attacks such reduced compounds.<sup>30</sup>

**EPR and UV/Vis/Near-IR Spectroelectrochemistry.** Both EPR and optical absorption spectroscopy are well suited to determine the nature of neighboring paramagnetic states of a complex with low-lying MLCT excited states. With respect to EPR, the unexpected result of these studies was the absence of any detectable signals for the one-electron oxidized form, even at 4 K. EPR spectra with rather small  $g$  anisotropy and  $^{195}\text{Pt}$  hyperfine coupling of  $\sim 5$  mT were observed for persistent hexacoordinate Pt(III) species with exclusively S or N heteroatom donors,<sup>9c-e,10d</sup> on the other hand, no EPR signals were reported for the square planar organometallic ion  $[(\text{Pt}(\text{C}_6\text{Cl}_5)_4)]^-$ .<sup>9a,b</sup> With  $2.57 \mu_B$  at room temperature, the magnetic moment for the latter complex ion<sup>9a</sup> already suggests that spin-orbit coupling effects contribute significantly to the ground and magnetically excited states of that  $5d^7$  species. Higher metal isotope coupling constants and much more pronounced  $g$  anisotropies were observed for Pt(III) centers, which can be generated via irradiation of single crystals containing "normal" Pt(II) salts; however, the exact structural situation of these centers with respect to the ligation at the unprotected axial sites is not known.<sup>10</sup>

In contrast to approximately octahedral low-spin  $d^7$  species, the corresponding square planar centers have several close-lying  $d$  orbitals to accommodate the electrons.<sup>39,40</sup> In addition to the large spin-orbit coupling constant of  $\sim 5000 \text{ cm}^{-1}$  for platinum,<sup>41</sup> this particular  $d$  orbital situation can cause very rapid EPR relaxation for species such as  $[\text{Pt}(\text{C}_6\text{Cl}_5)_4]^-$  or  $[(\widehat{N\ N})\text{PtMes}_2]^+$ . Additional evidence for this argument comes from a comparison with the low-spin  $d^7$  complex  $(\text{PEt}_2\text{Ph})_2\text{CoMes}_2$ , which has  $g_1$  3.72,  $g_2$  1.96 and  $g_3$  1.74,<sup>40a</sup> i.e., a large  $g$  anisotropy despite a much smaller spin-orbit coupling constant of  $\sim 500 \text{ cm}^{-1}$  for Co(II).<sup>41</sup> If there is a good analogy between  $[(\widehat{N\ N})\text{PtMes}_2]^+$  and

$(\text{PEt}_2\text{Ph})_2\text{CoMes}_2$ , the EPR silence of the former species would thus be not unexpected.

The analogy between square planar low-spin Co(II) and Pt(III) centers does indeed exist, as is obvious from UV/Vis/near-IR spectroelectrochemistry (Figure 9, Table 8). Three long-wavelength absorptions  $\lambda_{1-3}$  or  $\nu_{1-3}$  due to ligand-field (LF) transitions from doubly occupied  $d$  orbitals to the singly occupied  $d$  orbital are expected,<sup>39,40b,42</sup> e.g., for square planar low-spin Co(II) complexes such as  $(\text{PEt}_2\text{Ph})_2\text{CoMes}_2$ ,<sup>40b</sup> and are observed here for the electrogenerated Pt(III) complexes. The higher intensity of the LF transitions in case of the platinum complexes is due to the higher extent of orbital mixing in the  $5d^7$  relative to the  $3d^7$  situation; unfortunately, most reported optical spectra of transient Pt(III) species were restricted to the UV and visible regions.<sup>10,43</sup> Exact spectral assignments for square planar low-spin  $d^7$  systems are difficult to make,<sup>39,40b,42</sup> the strongest dependence of the second-lowest transition on the heterocyclic ligand suggests a tentative  $d$  orbital sequence  $(d_{xz})^2, (d_{x^2-y^2})^2, (d_{yz})^2, (d_z)^1$  for complexes  $[(\widehat{N\ N})\text{PtMes}_2]^+$  see Scheme 1).



All one-electron reduced complexes  $[(\widehat{N\ N})\text{PtAr}_2]^-$  exhibit EPR signals at room temperature which, however, are rarely sufficiently resolved to show ligand hyperfine structure (Figure 3, Table 3). The exception is the complex with  $\widehat{N\ N} = \text{dppz}$ , where the unpaired electron resides in the 1,4-diazine part of the molecule with little participation of the  $\alpha$ -diimine/metal site.<sup>30</sup> Despite being predominantly anion radical complexes of Pt(II),<sup>2e,6,8</sup> most anionic complexes exhibit a well-detectable rhombic  $g$  anisotropy in frozen solution (which explains the poor resolution of room-temperature spectra). This effect is favored both by the very large spin-orbit coupling factor of the  $5d$  metal and by the not totally negligible participation of platinum at the singly occupied MO (SOMO).<sup>8c</sup> This metal participation is also evident from the sizeable  $^{195}\text{Pt}$  isotope coupling, observed both in fluid solution and for the  $g_1$  and  $g_2$  components in the frozen state (Figure 1). The smallest metal splitting for the  $g_3$  component has similarly been observed for  $[(\text{bpy})\text{PtCl}_2]^-$  (Table 3).<sup>8c</sup> Small  $g$  anisotropies  $\Delta g$  were found for the complexes with the ligands bpm and dppz. The latter shows virtually no metal participation at the SOMO as evident from the virtually unchanged isotropic  $g$  factor relative to the value of 2.003 21 for  $\text{dppz}^{\cdot-}$ .<sup>30</sup> As mentioned before, the reason

(38) Ernst, S. D.; Kaim, W. *Inorg. Chem.* **1989**, *28*, 1520.

(39) Lever, A. B. P. *Inorganic Electronic Spectroscopy*, 2nd ed.; Elsevier Science Publishers: Amsterdam, 1984; p 503.

(40) (a) McKenzie, E. D.; Moore, R. D.; Worthington, J. M. *Inorg. Chim. Acta* **1975**, *14*, 37. (b) Falvello, L.; Gerloch, M. *Inorg. Chem.* **1980**, *19*, 472.

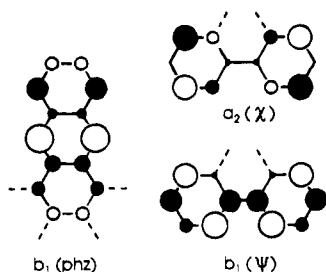
(41) Goodman, B. A.; Raynor, J. B. *Adv. Inorg. Chem. Radiochem.* **1970**, *13*, 136.

(42) For a discussion, see: Ceulemans, A.; Dendooven, M.; Vanquickenborne, L. G. *Inorg. Chem.* **1985**, *24*, 1159.

(43) (a) Goursot, A.; Chermette, H.; Waltz, W. L.; Lilie, J. *Inorg. Chem.* **1989**, *28*, 2241. (b) Goursot, A.; Chermette, H.; Waltz, W. L.; Lilie, J. *Inorg. Chem.* **1989**, *28*, 2247.

(44) Kaim, W. *J. Am. Chem. Soc.* **1982**, *104*, 3833.

for this effect lies in the occupation of an orbital  $b_1(\text{phz})$ , which is almost exclusively confined to the phenazine part of the molecule.<sup>30</sup>



The total amount  $\Delta g$  of  $g$  anisotropy (Table 3) thus shows a variation which is closely related to the extent of orbital interaction between the singly occupied  $\pi^*$  orbital of  $\widehat{\text{N}}\widehat{\text{N}}$  and the appropriate orbital ( $5d_{xz}$ ) at the metal. This interaction depends on the  $\pi^*$  orbital coefficients at the coordination centers, which are highest for bpz (and the related tap) ligand and lower for the bpm and bpm isomers.<sup>21</sup>

Except for the dppz complex where the metal participates very little at the SOMO, the  $g$  factors show a deviation to lower values relative to the free electron value  $g_e$  of 2.0023. According to an established concept,<sup>45</sup> this sign for the deviation of the isotropic  $g$  value suggests a frontier orbital situation with strong contributions from close-lying excited states with nonzero angular momentum involving low-lying *unoccupied* MOs, such as  $5d_{xy}$  or  $6p_z$ . In comparison, the contribution from those excited states involving *occupied* MOs such as the other  $5d$  orbitals should be small.

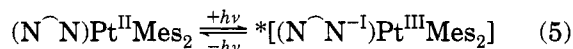
The relation  $g_{\parallel} > g_{\perp} > g_e > g_3$  is very different from the one expected for a square planar  $\text{Pt}(\text{I}) = 5d^9$  system, viz.,  $g_{\parallel} > g_{\perp} > g_e$ .<sup>46</sup> Nevertheless, the series of complexes  $[(\widehat{\text{N}}\widehat{\text{N}})\text{PtMes}_2]^-$  has allowed us to correlate the isotropic  $g$  factors with the metal isotope hyperfine splitting (Figure 4) as is often done successfully for metal-centered paramagnetic species.<sup>46,47</sup> A rather satisfactory linear correlation was obtained, the bpy complex showing the strongest effect due to a specific combination of  $\sigma$ -donor and  $\pi$ -acceptor capability. The anion  $[(\text{bpy})\text{PtMes}_2]^-$  also exhibits a lower  $g_{\text{iso}}$  than the  $\text{bpy}^{\cdot-}$  complexes of  $\text{PtPh}_2$ ,  $\text{Pt}(o\text{-CF}_3\text{Ph})_2$  and  $\text{PtCl}_2$ , indicating a closer situation of  $\pi^*$  ( $\widehat{\text{N}}\widehat{\text{N}}$ ) and low-lying unoccupied metal orbitals in the radical complexes with  $\text{PtMes}_2$ .

UV/Vis/near-IR spectroelectrochemistry of the anionic complexes confirms the notion of a predominant  $\widehat{\text{N}}\widehat{\text{N}}$  ligand-based electron uptake (eqs 3 and 4). The observed spectra (Figure 8, Table 7) show close similarity to those of the free ligand ions<sup>29–31</sup> and their complexes,<sup>30,48</sup> the spectra in the Vis/near-IR region of the radical complexes are dominated by intraligand ( $\pi \rightarrow \pi$ ) transitions which involve the SOMO. Many of these transitions show characteristic vibrational structuring; forbidden transitions that are very weak in the free ligands<sup>29,31</sup> gain in intensity after metal coordination.<sup>30,48</sup> While the absorption bands of the dimesitylplatinum complexes of the anion radical ligands show

slight hypsochromic shifts of  $\sim 1000 \text{ cm}^{-1}$  relative to those of free  $(\widehat{\text{N}}\widehat{\text{N}})^{\cdot-}$ , their similarity encourages us to transfer the previous assignments<sup>29,30,48</sup> to the complexes reported here. As has been noted previously for complexes of anion radicals,<sup>48</sup> the MLCT absorption bands which dominate the spectra of the precursor complexes are diminished in intensity and shifted into the UV region where they are often obscured by intense intraligand absorption bands. In most instances, the radical anions and their complexes exhibit transitions at longer wavelengths than the doubly reduced species (Figure 8, Table 7).

**Absorption and Emission Spectroscopy, Solvatochromism, and Reorganization Energies.** On the basis of the collected information on neighboring oxidation states we can interpret the optical absorption and emission spectra of the neutral complexes  $(\widehat{\text{N}}\widehat{\text{N}})\text{-PtMes}_2$  as follows.

In contrast to complexes  $(\widehat{\text{N}}\widehat{\text{N}})\text{M}(\text{CO})_4$ ,  $\text{M} = \text{Cr}, \text{Mo}, \text{W}$ ,<sup>21</sup>  $[(\widehat{\text{N}}\widehat{\text{N}})\text{Ru}(\text{bpy})_2]^{2+}$ ,<sup>38</sup> or  $[(\widehat{\text{N}}\widehat{\text{N}})\text{Cu}(\text{PPh}_3)_2]^+$ ,<sup>49</sup> the absorption spectra show generally structured bands (Figure 5) of medium intensity ( $\epsilon$  1500–4000  $\text{M}^{-1} \text{ cm}^{-1}$ ; Table 4) in the visible region. While part of this effect may be due to vibrational structuring in rather rigid complexes with low-coordinate metal centers, there appear to be several close-lying electronic transitions with comparable intensity. From the EPR and UV/Vis/near-IR spectroelectrochemical results (eqs 2–4), we can deduce that the lowest lying transitions should have MLCT character (eq 5).



The observed negative solvatochromism of the long-wavelength absorptions, i.e., their hypsochromic shift in more polar solvents (coupled with diminished structuring, Figure 7) is also indicative of “normal” MLCT transitions where the direction of the transition moment (metal to ligand) is opposite to the dipole moment in the ground state:  $(\widehat{\text{N}}\widehat{\text{N}})^{\delta+} - \text{Pt}^{\delta-}$ .<sup>24–28</sup>

Successful correlations with the  $E^*_{\text{MLCT}}$  parameters<sup>25</sup> (Table 6) also confirm the MLCT character underlying the long-wavelength band system; not only the direction but also the extent of the solvatochromism are typical for complexes between electron-rich metal centers and  $\pi$ -acceptor ligands<sup>24</sup> which are not engaging significantly in  $\pi/\pi$  interaction with solvent donor molecules.<sup>27</sup> The latter is due to the moderate acceptor character of complexes  $(\widehat{\text{N}}\widehat{\text{N}})\text{PtMes}_2$  and to the steric bulk of the mesityl groups, which precludes a  $\pi/\pi$  solvation interaction.<sup>27</sup> There is a small variation in the solvent sensitivity of the longest wavelength absorption feature which, however, is not without precedent;<sup>26,50</sup> the bpm complex exhibits the most pronounced such sensitivity whereas  $(\text{bpy})\text{PtMes}_2$  shows a relatively small solvatochromism. In comparison, the solvent sensitivity of  $\text{PtMes}_2$  complexes is smaller than that of  $\text{PtPh}_2$  analogues,<sup>26</sup> indicating a higher dipole moment in the ground state for the latter complexes with the less electron-rich diarylplatinum fragment. The band positions for individual solvents and the calculated inter-

(45) Kaim, W. *Coord. Chem. Rev.* **1987**, *76*, 187.

(46) Symons, M. *Chemical and Biochemical Aspects of Electron-Spin Resonance*; Van Nostrand Reinhold Co.: New York, 1978.

(47) Moscherosch, M.; Kaim W. *J. Chem. Soc., Perkin Trans. 2* **1992**, 1493.

(48) Braterman, P. S.; Song, J.-I.; Kohlmann, S.; Vogler, C.; Kaim, W. *J. Organomet. Chem.* **1991**, *411*, 207.

(49) Vogler, C.; Kaim W. *Z. Naturforsch.* **1992**, *47B*, 1057.

(50) Ernst, S.; Kurth, Y.; Kaim, W. *J. Organomet. Chem.* **1986**, *302*, 211.

cepts  $A$  at  $E_{\text{MLCT}}^* = 0.0$  (Table 6) show the expected and established<sup>21,38,49,50</sup> dependence on the  $\pi$ -acceptor ligands  $\widehat{N}\widehat{N}$ , which can also be deduced from the electrochemical potential differences  $E_{1/2}^{\text{oxI}} - E_{1/2}^{\text{redI}}$  (see below, Table 9).

In addition to the intense absorption bands with their irregular structuring, there are weak long-wavelength shoulders observable for each of the complexes  $(\widehat{N}\widehat{N})\text{PtMes}_2$  (Figure 5). These features may be attributed to <sup>3</sup>MLCT transitions which have sufficient intensity here because of the involvement of a heavy element.

Platinum(II) complexes show frequently emission from intraligand, MLCT, LF, or metal/metal excited states.<sup>5</sup> The complexes  $(\widehat{N}\widehat{N})\text{PtMes}_2$  offer the opportunity to study systems that exhibit systematically variable electronic structures and are shielded against aggregation or "direct" solvation in the first coordination sphere. On the other hand, the structural situation as indicated in Figure 1 is characterized by a certain rigidity which should not only improve the resolution of absorption features but also enhance the emission intensity due to the restriction of quenching processes.<sup>5</sup>

While a more detailed low-temperature emission study of some selected complexes  $(\widehat{N}\widehat{N})\text{PtMes}_2$  will be reported elsewhere,<sup>51</sup> the preliminary results of room-temperature luminescence in toluene solution summarized here (Figure 6, Table 5) already suggest that the typical emission bands with maxima between 580 and 620 nm result from MLCT excited states. In agreement with a hypsochromically shifted absorption, the compound  $(\text{bpy})\text{Pt}(\text{o-CF}_3\text{Ph})_2$  exhibits an emission band at 508 nm, i.e., at a much shorter wavelength than the dimesitylplatinum analogue. On the other hand,  $(\text{bpm})\text{PtMes}_2$  exhibits no detectable emission below 750 nm, as was also observed for  $(\text{bpm})\text{PtPh}_2$ .<sup>2e</sup> The reason for this latter result lies in the very low-lying MLCT excited state and in the facile quenching of this state by interaction with the peripheral nucleophilic  $\text{N}^{1,1'}$  centers.<sup>52</sup> Both the solvatochromism of the emission maximum of  $(\text{bpy})\text{PtMes}_2$  and the decreasing Stokes shift for the complexes with better  $\pi$ -acceptor ligands suggest an emission from a <sup>3</sup>MLCT excited state, as was discussed previously for related systems.<sup>5a,o,q</sup>

The availability of both oxidation and reduction potentials for complexes with low-lying MLCT absorption and emission has allowed us to correlate (eq 6) the

$$\Delta E = E_{1/2}^{\text{oxI}} - E_{1/2}^{\text{redI}} \text{ (in V)} = E_{\text{op}} \text{ (in eV)} - \chi \quad (6)$$

electrochemical differences  $\Delta E$  with the optical data. Such correlations have been obtained before for ruthenium(II) "polypyridine" complexes<sup>53</sup> and some other complexes of  $d^8$  metals.<sup>54</sup> Here we report a first such correlation with calculated contributions  $\chi$  from inter- and intramolecular reorganization<sup>55</sup> for a series of  $d^8$ -configured systems in two different solvents (Table 9).

**Table 9.** Correlation<sup>a</sup> between Optical and Electrochemical Data for Complexes  $(\widehat{N}\widehat{N})\text{PtMes}_2$  in Two Different Solvents

$\widehat{N}\widehat{N}$	$\Delta E = E_{1/2}^{\text{oxI}} - E_{1/2}^{\text{redI}}$ (V)		$E_{\text{op}}$ (eV) <sup>b</sup>		$\chi$ ((eV)) <sup>b</sup>	
	THF	MeCN	THF	MeCN	THF	MeCN
bpy	2.37	2.27	2.58	2.67	0.21	0.43
bpm	1.90	1.78	2.09	2.22	0.20	0.44
bpz	2.06	1.99	2.31	2.37	0.25	0.38
bpym	2.21	2.11	2.45	2.57	0.24	0.46
tap	2.09	1.98	2.31	2.41	0.22	0.43
dppz	1.99	1.91	2.51	2.67	0.52	0.76

<sup>a</sup>  $\chi = E_{\text{op}} - \Delta E$ . <sup>b</sup> 1 eV = 8065.5  $\text{cm}^{-1}$ .

### Scheme 1

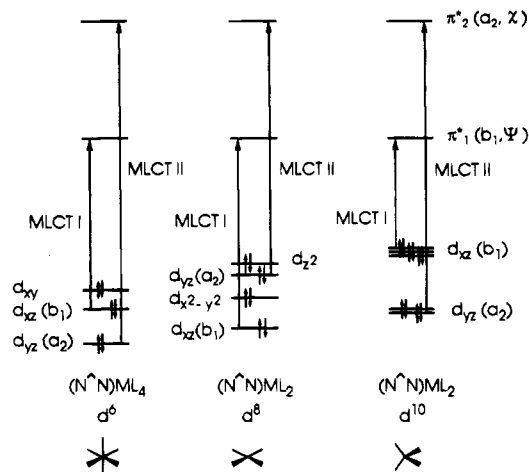


Table 9 shows that the reorganization energies are generally larger by  $\sim 0.2$  eV in the more polar acetonitrile (intermolecular contribution) than in THF, where most values  $\chi$  are similar to the  $\chi \sim 0.2$  V obtained for complexes of  $[(\widehat{N}\widehat{N})_2\text{Ru}]^{2+}$ .<sup>53</sup> This result indicates both a fairly high degree of conformational rigidity due to steric crowding (Figure 1) and little geometrical restructuring in going from  $(\widehat{N}\widehat{N})^0$  to  $(\widehat{N}\widehat{N})^-$  and from Pt(II) to Pt(III) (intramolecular contributions to  $\chi$ ). Large deviations of  $\chi > 0.5$  (eV) are observed and expected<sup>15,30</sup> for the dppz complex because the "redox orbital"  $b_1(\text{phz})$  is different from the "optical orbital"  $b_1(\psi)$  in this case.

An excellent correspondence between optical and electrochemical data is obtained when information from absorption and emission in the same solvent are combined. For  $(\text{bpy})\text{PtMes}_2$  in MeCN, the average between the absorption maximum at 2.67 eV ( $21\,505\text{ cm}^{-1}$ , 465 nm) and the emission maximum at 1.75 eV ( $14\,140\text{ cm}^{-1}$ , 707 nm) lies at 2.21 eV and thus very close to the  $\Delta E$  value of 2.27 V in that solvent (Table 9).

In view of all available information from electrochemistry and EPR and UV/Vis/near-IR spectroscopy of complexes  $[(\widehat{N}\widehat{N})\text{PtMes}_2]^n$ , we can assign the absorption spectra of the neutral forms as follows: The weak long-wavelength shoulders of the main intense band system are due to <sup>3</sup>MLCT transitions, which owe their visibility to the presence of a  $5d^8$  metal center. The highly solvatochromic and always structured group of absorptions in the visible and near-UV region involves apparently two <sup>1</sup>MLCT absorption band systems which exhibit vibrational splitting. Whereas the resolution of vibrational splitting in nonpolar solvents is favored by the low coordination number of the  $d^8$  system<sup>56</sup> and by

(51) Stückl, A. C.; Klein, A., in preparation.  
 (52) Kaim, W.; Matheis, W. *Chem. Ber.* **1990**, *123*, 1323.  
 (53) Dodsworth, E. S.; Lever, A. B. P. *Chem. Phys. Lett.* **1985**, *119*, 61; **1986**, *124*, 152.  
 (54) (a) Bruns, W.; Kaim, W.; Waldhör, E.; Krejčík, M. *Inorg. Chem.*, in press. (b) Kaim, W.; Bruns, W.; Kohlmann, S.; Krejčík, M. *Inorg. Chim. Acta* **1995**, *229*, 143.  
 (55) Kober, E. M.; Goldsby, K. A.; Narayana, D. N. S.; Meyer, T. J. *J. Am. Chem. Soc.* **1983**, *105*, 4303.

(56) Ladwig, M.; Kaim, W. *J. Organomet. Chem.* **1992**, *439*, 79.

the geometrical rigidity, the closeness of both overlap-favored MLCT transitions MLCT1 ( $d_{yz} \rightarrow \pi^*_1(\psi)$ ) and MLCT2 ( $d_{xz} \rightarrow \pi^*_2(\chi)$ ) is due to an orbital situation (Scheme 1) where the  $d_{xz}$  orbital lies *lower* than  $d_{yz}$ .

This situation is thus different from that of essentially octahedral complexes  $(\widehat{N})ML_4$  of  $d^6$  metal centers<sup>21,57</sup> and from that of approximately tetrahedral complexes  $(\widehat{N})ML_2$  of  $d^{10}$  metals,<sup>49</sup> where the differences between MLCT1 and MLCT2 are much larger.

---

(57) Balk, R.; Stufkens, D. J.; Oskam, A. *Inorg. Chim. Acta* **1978**, *28*, 133.

**Acknowledgment.** This work was supported by Deutsche Forschungsgemeinschaft (SFB 270), Volkswagen-Stiftung, and Fonds der Chemischen Industrie. We thank J. Fees for the dppz ligand.

**Supplementary Material Available:** Table of reaction times, yields, and elemental analyses for complexes  $(\widehat{N})Pt(Mes)_2$  (1 page). Ordering information is given on any current masthead page.

OM9406097